Journal of Port and Harbor Research. RIPAH
Korea Maritime University Vol. 8. pp. 169~176. 1997.

論 文

Ocean Wave Analysis around Ship and Numerical Review

*K. H. Sohn** · *S. H. Kwag***

선체주위의 해양파 해석 및 수치적 고찰

손 경 호 · 곽 승 현

Key Words : Ocean Waves(해양파), Free Surface(자유표면), Viscous Flows(점성유동), Boundary Condition(경계조건), Triple Mesh(3중격자), Grid Size(격자크기), Multi Grid(복합격자)

Abstract

To analyze the ocean wave more efficiently, more fine grids are used with relatively less computer memory. Each element of free surface is discretized into more fine grids because the ocean waves are much influenced by the mesh used in the finite difference scheme. According to the flow analysis, remarkable improvements could be seen in the free surface generation. The multi grid is applied to confirm the validity of scheme. The Baldwin Lomax turbulence model is used for the analysis of S103 Inuid ship. Finally some discussion on experiments was made for the physical phenomena of the viscous flows around ship.

1. Introduction

The finite difference method has a serious problem because it requires very long CPU time and a huge memory storage for accurate simulation. Recently, the improvement of the efficiency has been strongly demanded. The method of implicit scheme is one of the examples for more efficient computations. Some comparative calculations by that method has been carried out. It seems that IAF(1) is quite promising to speed up the calculation but its formulation is a little complicated. For the numerical truncation error to be small enough to have little effect on the

* 한국해양대학교 선박해양공학부 교수
** 한라공과대학교 조선공학과

physical performance, the mesh size should be strictly considered. The mesh size must be extremely small for high Reynolds-number flows to meet this demand. However, such fine meshes are not always necessary for all the equations and terms. For example, the truncation errors of the Poisson equation for the pressure of the non-convective terms in Navier-Stokes equation do not have much influence on the results as the convection terms do. The hybrid type of the mesh may make the computations more efficient. One possibility is to employ different mesh systems depending on the characteristics of the equations or the terms. We call such a method "double mesh method(2)" or "triple mesh method(3)", written in short as DMM or TMM hereafter. It was first proposed for numerical simulations of 3-D nonlinear free-surface flow problems by boundary element method(4). In order to reduce the numerical viscosity as much as possible, a very fine mesh system which contains about 60 grids(5) in one wave length is used in the finite difference calculation concerned with the free-surface equations, while the governing Laplace equation is solved on a relatively coarse mesh system which contains about 10 grids in one wave length by the boundary element method.

The computed results by DMM or TMM were of enough accuracy and both the computing time and the size of the memory storage were remarkably reduced. In the present paper, a multi-grid on the free-surface is introduced in the finite difference solver of the Navier-Stokes equation to improve the calculation efficiency. As mentioned, the demands to the mesh size are not the same for all the equations and the terms in the finite difference method. So it is expected that some improvement, similar to that achieved in the simulation of free-surface problem by DMM or TMM, may be made by introducing more fine meshes in the conventional finite difference scheme.

2. Numerical Strategy

2.1 Basic Equation

The grid size for the calculation of the free-surface elevation must be determined by a different scale, the minimum wave length. A single grid system(6) is usually used in the whole computation whose minimum size is determined for the numerical diffusion to be less than that by viscosity. In the simulation, two or three mesh systems are usually used whose sizes are different each other depending on the characteristic of equations. The first is for the convective terms in the Navier-Stokes equation, the second is for the Poisson equation, and the third is for the free-surface equation. The third grid system requires the finest mesh. In the present calculation, the third one is numerically confirmed ; more fine grids are used to improve the accuracy of free-surface calculation with relatively less computer storage. One element of the free-surface is discretized into (4xii,4xjj), (8xii,4xjj), (12xii,4xjj) fine grids because the free-surface waves are much affected by the grid size in the finite-difference scheme. Fig. 1 shows the shape of (4xii,4xjj) discretization.

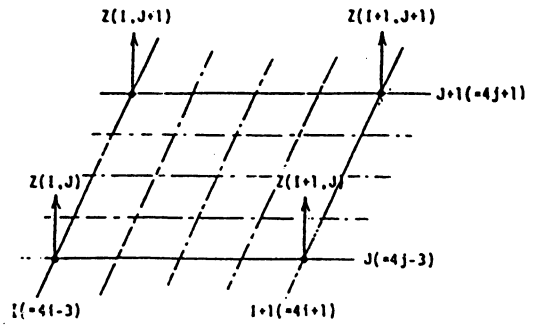

Fig. 1 Discretization of grid on free-surface (4xii,4xjj case)

The positions, or Lagrangian coordinates, of each particle (x^n_p,y^n_p,z^n_p) are obtained by numerical integration from some initial position (x^0_p,y^0_p,z^0_p) at time t=0;

$$\begin{aligned} x^n_p &= x^0_p + \int^t u_p \cdot dt \\ y^n_p &= y^0_p + \int^t v_p \cdot dt \\ z^n_p &= z^0_p + \int^t w_p \cdot dt \end{aligned} \quad \cdots\cdots (1)$$

where u_p,v_p,w_p are the velocities in the Eulerian mesh at the time dependent location of the particle. In the present MAC-based codes, the particle velocities are evaluated by two-variable linear interpolation. Consistently with the forward time integration of MAC method, (1) is evaluated sequentially as (2).

$$\begin{aligned} xi^{n+1} &= xi^n + ui^n \cdot \triangle t \\ yi^{n+1} &= yi^n + vi^n \cdot \triangle t \\ zi^{n+1} &= zi^n + wi^n \cdot \triangle t \end{aligned} \quad \cdots\cdots (2)$$

(2) is the Lagrangian expression of the kinematic condition on the free-surface. The condition can also be expressed in the Euler form as follows;

$$\partial\zeta/\partial t = -u \cdot \partial\zeta/\partial x - v \cdot \partial\zeta/\partial y + w \quad \cdots\cdots (3)$$

where ζ and t are the free-surface elevation and the time respectively. Numerically (2) is equivalent to (3) if the 1st order upstream difference scheme is used in (3).

The shape of the free-surface is not known a priori; it is defined by the position of the marker particles. We note here that the boundary conditions at the free-surface require zero tangential stress and a normal stress which balances any externally applied normal stress. The application of these conditions requires a knowledge of not only the location of the free-surface at each grid but also its slope and curvature. In our calculation, the z-coordinate of the free surface is re-arranged by the bivariate linear interpolation in proportion to the newly calculated projected area at each time-step.

2.2. Lagrangian Expression of Kinematic Free Surface Condition

Suppose $P_{i-1}(X_{i-1},Z^n_{i-1})$ and $P_i(X_i,Z^n_i)$ are two grids on the free surface at t=n as shown in Fig. 2. At the next time step t=n+1, these mark points move to $P'_{i-1}(X'_{i-1},Z'_{i-1})$ and $P'_i(X'_i,Z'_i)$ respectively.

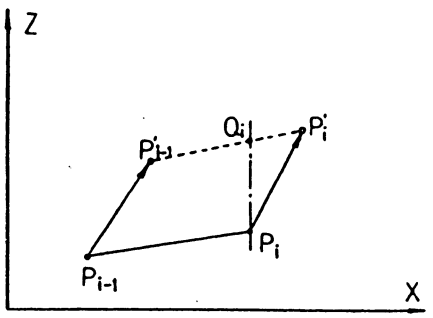

Fig. 2 Free surface movement

In the present research, the x,y coordinates of the grids on the free surface are fixed and z coordinate moves freely. The elevation of the new free surface grid Q_i can be determined by P'_{i-1} and P'_i as follows;

$$\zeta_i{}^{n+1} = z_i' + k \cdot (Xi - Xi') \quad \cdots\cdots (4)$$

where

$$\begin{aligned} k &= (Z_i' - Z_{i-1}')/(X_i' - X_{i-1}') \\ &= \{Z_i^n - Z_{i-1}^n + (w_i^n - w_{i-1}^n) \cdot \Delta t\} \\ &\quad / \{x_i - x_{i-1} + (u_i^n - u_{i-1}^n) \cdot \Delta t\} \end{aligned} \quad \cdots\cdots (5)$$

ξ_i^{n+1} can be further expressed as

$$\begin{aligned} \zeta_i{}^{n+1} &= \zeta_i{}^n + w_i^n \cdot \Delta t \\ &\quad - (u_i^n \Delta t) \cdot (\zeta_i{}^n - \zeta_{i-1}{}^n)/(x_i - x_{i-1}) \\ &\quad \cdot \{1 + (\Delta w/\Delta x)\Delta t\} / \{1 + (\Delta u/\Delta x)\Delta t\} \end{aligned} \quad \cdots\cdots (6)$$

or

$$(\zeta_i^{n+1} - \zeta_i^n)/\Delta t = w_i^n - u_i^n \cdot (\zeta_i^n - \zeta_{i-1}^n)/\Delta x \cdot \{1+(\Delta w/\Delta x)\Delta t\} / \{1+(\Delta u/\Delta x)\Delta t\} \quad \cdots (7)$$

where

$$\Delta w/\Delta x = (w_i^n - w_{i-1}^n)/(x_i - x_{i-1}) \quad \cdots (8)$$
$$\Delta u/\Delta x = (u_i^n - u_{i-1}^n)/(x_i - x_{i-1})$$

2.3 Turbulence Model

The turbulence model is Baldwin- Lomax [9] zero equation model, whose original form is from Cebeci-Smith[10].

It is widely used in the aerodynamic computational and also in the incompre-ssible flow computation around ship. In the present study, flow is enforced to be turbulent from the fore of a ship. The free-surface effect on turbulence is not included in the model. There has not been any turbulence model that can be applied to the boundary layer and wake of a surface piercing body like a ship. Therefore in the present calculation, the simple zero equation model is used. The kinematic eddy viscosity is evaluated in the inner and outer layers separately.

3. Computation and Discussion

To confirm the numerical efficiency of the multi grid, the high Reynolds-number free surface wave of S-103 is studied. S-103 is an Inuid model with the beam/length ratio of 0.09. In the present case, calculations are made at $Rn=10^6$ and Fn=0.28 with Baldwin-Lomax turbulence model. The result is that at the time T=3.0, when the convergence is well assured. The grid size of regular type is 74x29x30 and the multi-grid on the free-surface is numerically tried. Fig.3 shows the wave patterns obtained by the regular grid. Fig.4 uses the grid of (4xii,4xjj) on free surface and gives us about 7% improvement in the free surface development, compared with that by regular grid. It means that the size of grid is very important in moving the marker particles on free surface. Fig.5 uses that of (8xii,4xjj) on free surface. It shows the improvement of about 19% at T=3.0. Fig.6 uses that of (12xii,4xjj) on free surface. Some more improvement is obtained; 29% compared with that of regular grid at T=3.0.

Fig. 7 shows a significant wave patterns although the Froude number changes modestly from 0.26 to 0.30; at Fn=0.27 no significant stern wave is observed compared with those at Fn=0.26 or 0.28. On the other hand, a wide "wake" zone in Fig.8 is observed behind the hull at Fn=3.0. A careful observation of the "wake" tells us that the free surface wave fluctuates intensively there. The free surface at Fn=0.27 is completely different where such free surface fluctuation is not observed. The separation of Fn=0.27 takes place at more upstream position than that of Fn=0.30. This situation can be seen more clearly in the limiting streamlines in Fig. 9. The separated region of Fn=0.27 is significantly wider than that of 0.30. The experiments by twin tufts show similar tendency; the separated region of Fn=0.30 close to the free surface is due to the free surface sub-breaking.

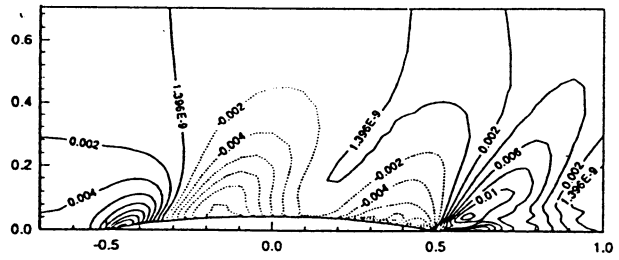

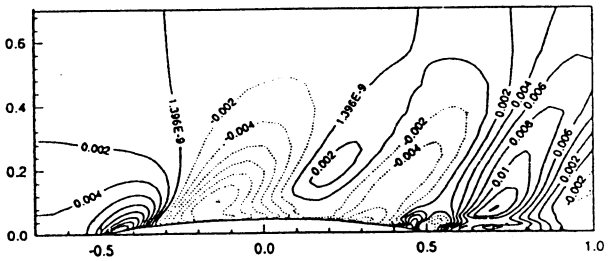

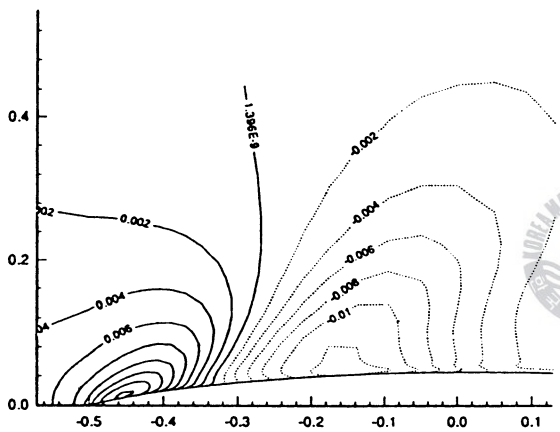

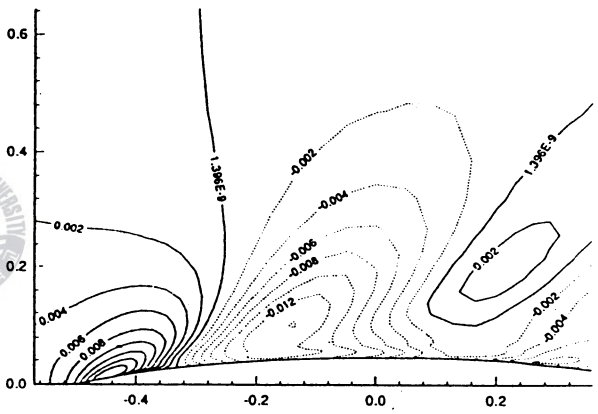

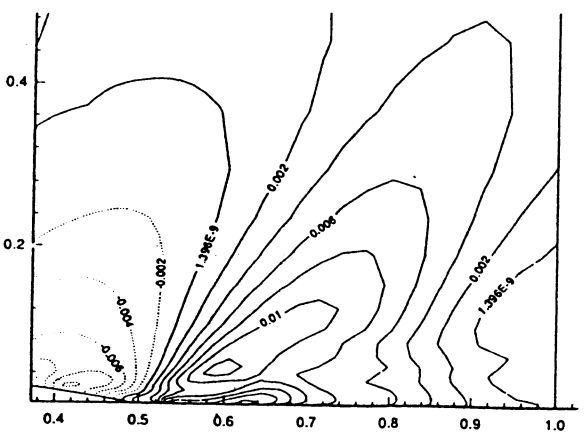

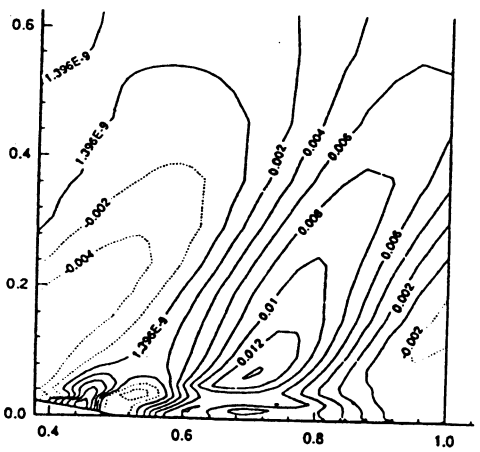

Fig. 3 Free surface contour by regular grid (ii,jj) for S-103 case

Fig. 4 Free surface contour by multigrid (4xii,4xjj) for S-103 case

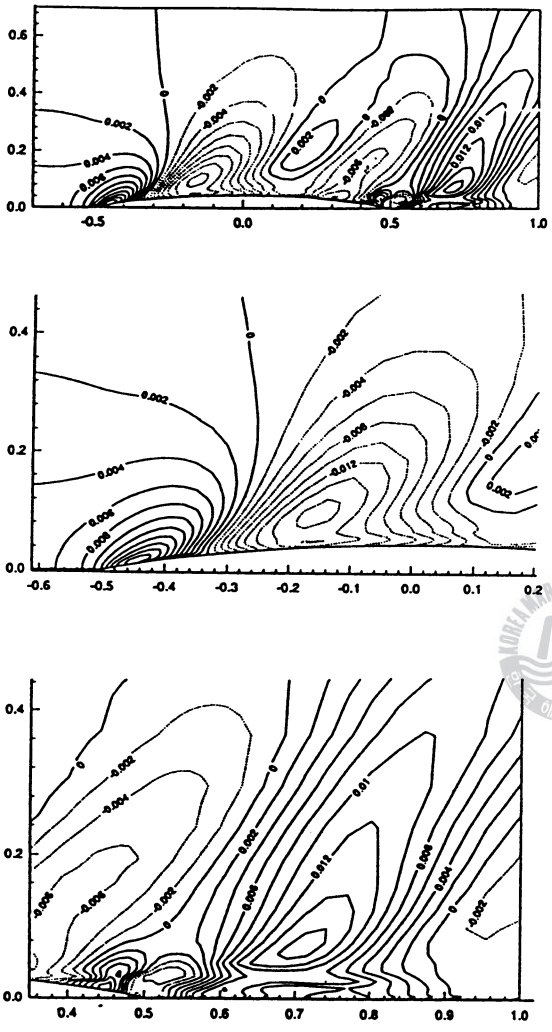

Fig. 5 Free surface contour by multi grid (8xii,4xjj) for S-103 case

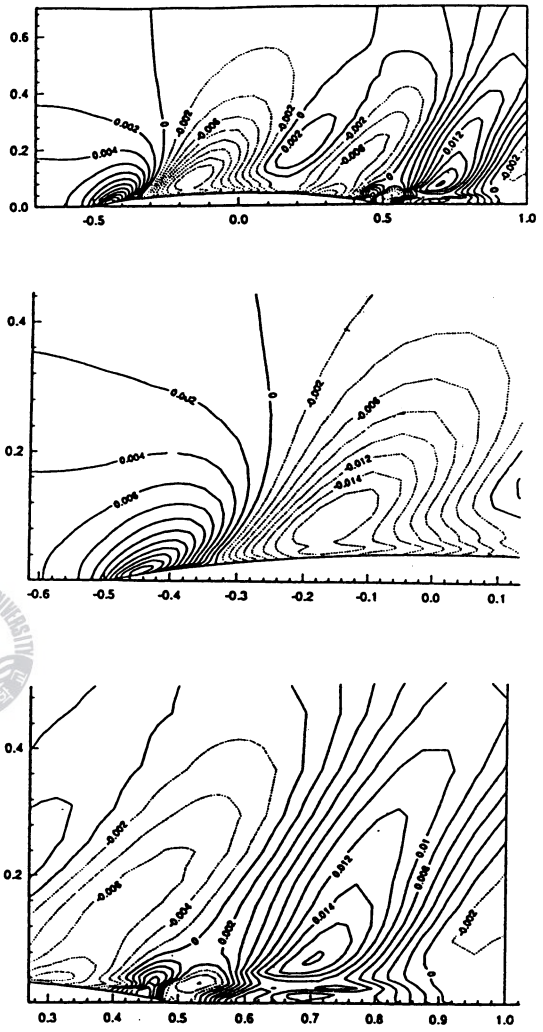

Fig. 6 Free surface contour by multi grid (12xii,4xjj) for S-103 case

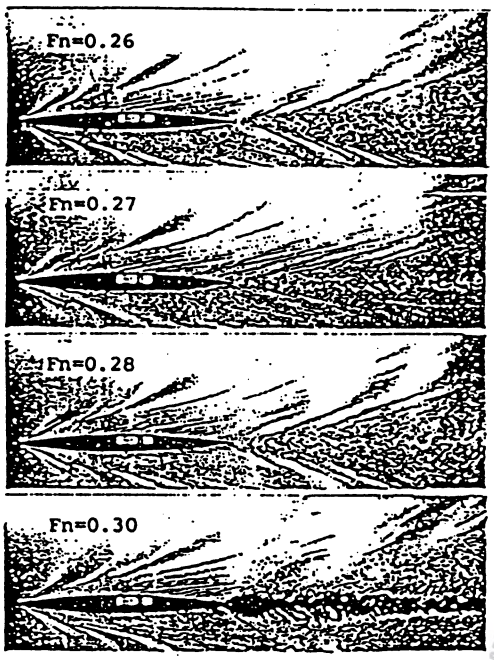

Fig. 7 Wave patterns of S-103 at four different Froude numbers

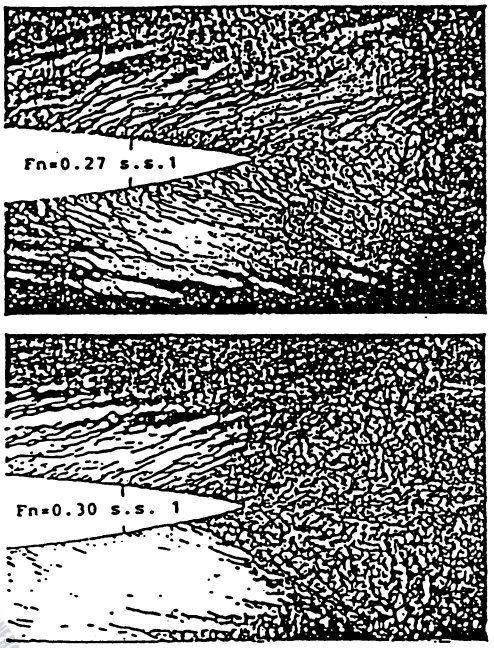

Fig. 8 Stern wave pictures of S-103 at Fn=0.27 and 0.30

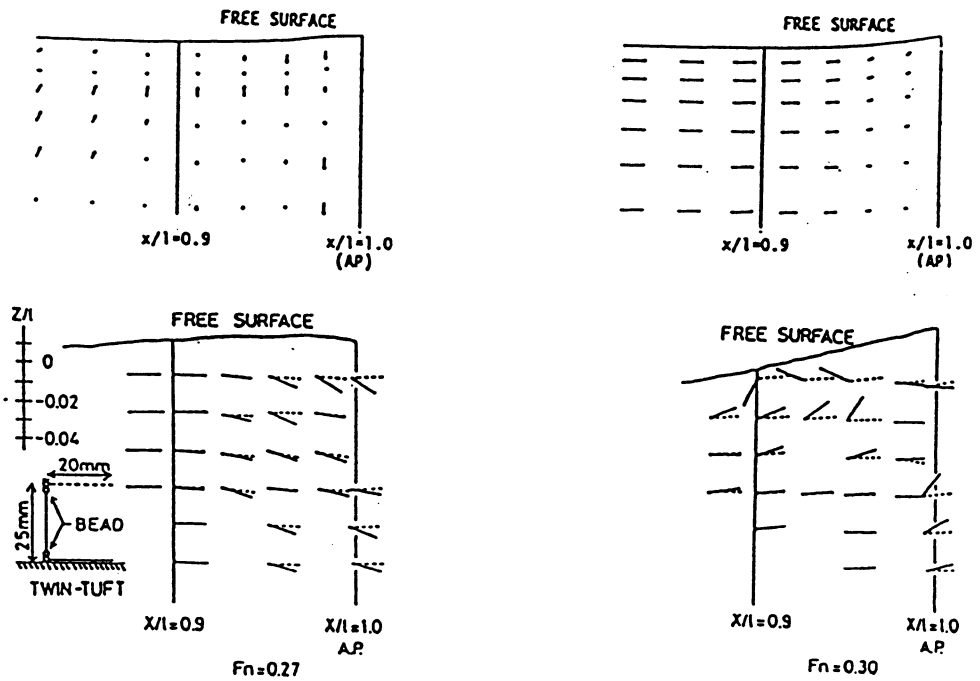

Fig. 9 Calculated (above) and observed(below) limiting streamlines at Fn=0.27 and Fn=0.30

4. Conclusion

To simulate the free surface wave more efficiently, the multi-grid method is applied to the finite difference solution of Navier-Stokes equation. The method is to use the multi grid system on the free surface. Through several comparative computations, we found that the method is significantly effective for the free surface simulation of the viscous flows. Finally some discussions on experiments are made for the physical phenomena of the viscous flows around ship.

요 약

항만공학 분야의 해양파 문제에서 자유수면파를 수치 및 실험에 의한 방법으로 해석하였다. 수치적인 방법은 자유수면 격자를 유한차분법의 이산화 과정을 통해 精度를 향상시키기 위하여 나비에 스토크스 방정식의 각항에 서로 다른 형태의 격자를 적용하여 컴퓨터의 용량을 최소화하고 수렴속도를 극대화하는 것이다. 난류흐름을 재연하기 위해 Baldwin Lomax 모형을 도입하였고 대상모형은 S103 선박으로 하였다. 실험은 프루드수 0.26부터 0.30까지 수행하였고 각 속도마다 조파현상을 해석해서 수치결과와 비교하였다. 본연구는 해양파의 점성유동장 해석에서 복합격자를 사용했을때의 수치계산 결과가 실험값에 접근하고 있음을 보여주고 있다.

5. References

1) Kodama,Y., "Computation of High Number Flows past a Ship Hull Using the IAF Scheme", Jour of Soc of Naval Arch of Japan, Vol.161,1987

2) Xu,Q., Mori,K., Shin,M., "Double Mesh Method for Efficient Finite Difference Calculation", Jour of Soc of Naval Arch of Japan, Vol.166, 1989

3) Mori,K., Kwag,S., Doi,Y., "Numerical Simulation of Ship Wave and Some Discussions on Bow Wave Breaking and Viscous Interaction of Stern Wave", 18th Symp on Naval Hydrodynamics, U.S.A.,1990

4) Xu,Q., Mori,K., "Numerical Simulation of 3-D Nonlinear Water Wave by Boundary Element Method", Jour of Soc of Naval Arch of Japan, Vol.165,1989

5) Shin,M., Mori,K., "Numerical Computation of 2-D Waves behind a Hydrofoil", Jour of Soc of Naval Arch of Japan, Vol.163,1988

6) Hino,T., "Numerical Computation of a Free Surface Flow around a Submerged Hydrofoil by the Euler/Navier-Stokes Equations", Jour of Soc of Naval Arch of Japan, Vol.164,1988

7) Kwag,S.H., Mori,K., Shin,M., "Numerical Computation of 3-D Free Surface Flows by N-S Solver and Detection of Sub-Breaking", Jour of Soc of Naval Arch of Japan, Vol.166,1989

8) Mori,K., Kwag,S.H., Doi,Y., "Numerical Simulation of "Ship Waves and Some Discussions on Bow Wave Breaking & Viscous Interaction of Stern Waves", 18th Symp on Naval Hydro.,USA, 1990

9) Baldwin,B., Lomax,H., " Thin - Layer Approximation and Algebraic Model for Separated Turbulent Flows", AIAA paper 78-257,1978

10) Cebeci,T., Smith,A.M.O., "A Finite Difference Method for Calculating Compressible Laminar and Turbulent Boundary Layers", Jour. Basic Eng., Trans. of ASME, pp.523-535, 1970